Int. J. Heat Mass Transfer. Vol. 21, pp. 605–613

0017-9310/78/0501-0605 $02.00/0

HEAT TRANSFER CHARACTERISTICS OF EVAPORATION OF A LIQUID DROPLET ON HEATED SURFACES

ITARU MICHIYOSHI† and KUNIHIDE MAKINO‡

(*Received* 3 *June* 1977)

Abstract—This paper presents heat-transfer characteristics of evaporation of a single droplet of pure water placed on smooth surfaces of copper, brass, carbon steel and stainless steel at temperature ranging from 80 to 450°C. From time-dependent measurements of surface temperature just below the droplet and those of change in geometrical shape of droplet, we can obtain the time-averaged heat flux q and the surface temperature T_{ws}. The heat-transfer characteristics are analysed by correlating the heat flux q with $\Delta T_{sat} = T_{ws} - T_{sat}$. From this boiling curve, it is found that the present data in the nucleate boiling region come on a certain line parallel to the nucleate pool boiling curve for thin water film, no matter what materials are used for heated plate, while in the film boiling region, the theoretical curve derived by Baumeister *et al.* does not always agree with the present data. And new formulae are presented for predicting more well the film boiling curve. The transition boiling is also discussed.

NOMENCLATURE

A, projected base area of droplet [m²];
$\bar{A}$, time-averaged projected base area of droplet [m²];
D, diameter of droplet at any time [m];
D_0, initial diameter of droplet [m];
L, latent heat of vaporization [J/kg];
L_0, enthalpy difference between initial droplet and of saturated water [J/kg];
L^*, reduced latent heat of vaporization [J/kg] $L^* = L[1+(7/20)c_{pv}(\Delta T_{sat}/L)]^{-3}$;
T_B, temperature T_{w0} at the beginning of bubble formation [°C];
T_F, temperature T_{w0} having the maximum evaporation time, i.e. Leidenfrost temperature [°C];
T_M, temperature T_{w0} having the minimum evaporation time [°C];
T_{sat}, saturation temperature [°C];
T_w, surface temperature just below droplet at any time [°C];
T_{w0}, initial surface temperature [°C];
T_{ws}, time-averaged surface temperature [°C];
T_l, liquid temperature of droplet [°C];
ΔT, $= T_w - T_l$ [K];
ΔT_{drop}, maximum temperature difference between T_{w0} and T_w [K];
ΔT_{sat}, $= T_{ws} - T_{sat}$ [K];
Q, heat required to evaporate completely one droplet [J];
V, volume of droplet at any time [m³];
V_0, initial volume of droplet [m³];
a, function of T_{w0}, in equation (5);
c_{pv}, specific isobaric heat capacity of steam [J/(kg·K)];
g, acceleration of gravity [m/s²];
n, function of T_{w0}, in equation (5);
q, time-averaged heat flux [W/m²];
t, time [s];
t^*, reversed time, its origin is the time when the droplet just disappears [s].

Greek symbols

α, heat-transfer coefficient between surface and droplet at any time [W/(m²·K)];
$\bar{\alpha}$, time-averaged α [W/(m²·K)];
δ, thickness of thin water film [m];
κ, thermal diffusivity of surface material [m²/s];
λ, thermal conductivity of surface material [W/(m·K)];
λ_v, thermal conductivity of steam [W/(m·K)];
μ_v, viscosity of steam [Pa·s];
ρ, density of pure water [kg/m³];
ρ_v, density of steam [kg/m³];
τ, total evaporation time [s].

INTRODUCTION

THE INFORMATION on the heat-transfer characteristics of a liquid droplet on a heated surface is currently important in safety considerations of various types of reactors. At the present time, there are many works related to the evaporation of a single droplet. But the most works are concerned with the "Leidenfrost point" and/or with the temperature range higher than that point. In this temperature range, many analytical models from a small droplet to a larger one are presented with various assumptions. They derive theoretical or semi-empirical equations to calculate the heat-transfer characteristics of the droplet, such as evaporation times and coefficients of heat transfer and so on [1–3, 12]. Those calculated values do not always agree with experimental data, as will be shown later.

† Department of Nuclear Engineering, Kyoto University, Kyoto, Japan.
‡ Department of Mechanical Engineering, Maizuru Technical College, Maizuru, Kyoto, Japan.

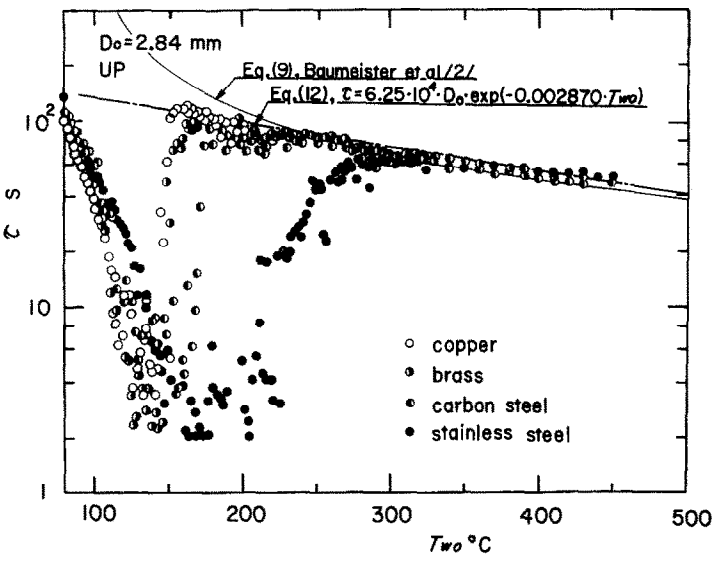

FIG. 1. Total evaporation time τ vs T_{w0}.

Baumeister *et al.* [4] presented the prediction technique of "Leidenfrost point" by considering effects of the critical temperature of the liquid, thermal properties of the solid, surface energy of the liquid, and surface energy of the solid. But considerable differences exist between those predicted "Leidenfrost point" and the experimental data obtained by many research workers. And other investigators [5, 6] discussed about the dynamic instability of droplet.

Recently Emmerson [7] conducted an experimental study, dealing with effects of pressure and surface material on the "Leidenfrost temperature, T_F," and the temperature range over it. It is full of interest that he paid as much attention to the wettability and thermal diffusivity of surfaces as to heat-transfer characteristics of a droplet. On the other hand, there are few works in the temperature range lower than T_F point. In this temperature range only Hiroyasu *et al.* [3] investigated the evaporation of droplet of various liquids.

To find out experimentally the heat-transfer characteristics of a droplet, we must conduct time-dependent measurements of the projected base area A of a droplet and of the surface temperature T_w just below it and the liquid temperature T_L within it. The projected base area A and volume of droplet were measured in the temperature range higher than T_F by Gottfried *et al.* [1] and Wachters *et al.* [12], respectively. Measurements of the surface temperature T_w were conducted [8, 9], using the surface made of stainless steel together with various organic liquids as well as water. The former used the chromel–alumel thermocouple of 50 μm dia and the latter the resistance thermometer of thin film nickel. No measurement of liquid temperature T_L of a droplet has ever been made.

When a single pure droplet having the same size is settled on a heated surface, the total evaporation time τ of a droplet, arranging it with the initial surface temperature T_{w0}, varies mainly with the materials and conditions of the surfaces. In case of different surface materials and the same surface treatment, one example of the present experimental results of total evaporation time τ is shown in Fig. 1. It shows that the evaporation time τ is considerably affected by the surface materials in the range lower than T_F, while it is not different in the range higher than T_F temperature, which has relations to the thermal diffusivities of each surface material as shown in Fig. 2. In Fig. 1, the theoretical curve of Baumeister *et al.* [2], which can be calculated taking into account the change in volume of droplet, is also drawn. It can be seen that the theory does not always agree with the experimental data, as already mentioned.

This paper presents the heat-transfer characteristics of evaporation of a small droplet of pure water settled on the various heated plates (materials: copper, brass, carbon steel and stainless steel) at the initial surface temperature T_{w0} ranging from 80–450°C. The initial temperature of droplet is about 20°C. Two thermocouples are made use of for the time-dependent

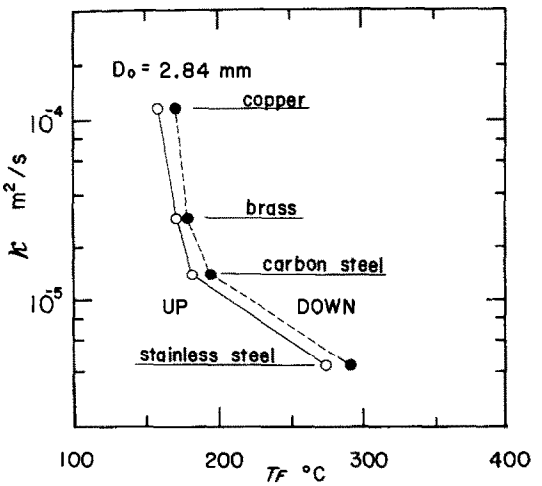

FIG. 2. Thermal diffusivity of plate vs Leidenfrost temperature.

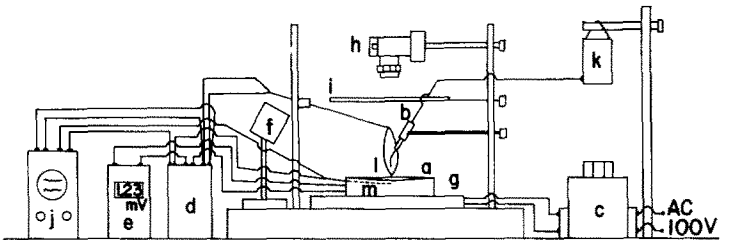

FIG. 3. Schematic diagram of apparatus: a, heated surface; b, hypodermic syringe; c, variac; d, cold junction; e, digital-volt-meter; f, strobo-scope; g, heating unit; h, strobo-streak camera or 8 mm cine-camera; i, glass; j, dual-beam synchroscope; k, water tank; l, 25 μm diameter thermocouple; m, 0.3 mm diameter thermocouple.

measurements of surface temperature T_w just below the droplet and of liquid temperature T_L within the droplet. Change in geometrical shape of a droplet on the heated plate is recorded by strobo-streak camera and 8 mm cine-camera. From these measurements we can calculate the time-averaged heat flux q and the time-averaged surface temperature T_{ws}, and then we discuss the so-called boiling curve of a single droplet on the heated plate. To the authors' knowledge, such a boiling curve has not yet been obtained.

EXPERIMENTAL APPARATUS AND PROCEDURE

In the range of temperature T_{w0} less than T_F, we use a droplet of water of 3.29 mm dia and four plates of various materials (copper, brass, carbon steel and stainless steel). These plates, having the same size of 50 mm dia and 20 mm thickness, are engraved with a very small groove on the surface from the edge to the center. In this groove a 0.3 mm dia chromel–alumel sheath type thermocouple is buried with solder. The surface soldered along the groove is planed and finished until the sheath of the thermocouple is almost bared. At room temperature the whole surface of the plate is polished with chrome oxide to a mirror finish and then carefully cleaned by benzene. The surface thus treated is used for heat-transfer experiments at any temperature T_{w0}, which are conducted stepwise from room temperature to higher temperature, which is called UP, and thereafter are conducted again stepwise from that high temperature to room temperature, which is called DOWN. In such a way, the surface is rusted slowly, and the wettability increases.

In the range of temperature T_{w0} higher than T_F, in order to study effects of the initial droplet size D_0 on the heat-transfer characteristics, we use four initial droplet sizes, 2.54, 2.78, 2.86 and 3.29 mm dia, and two plates made of copper and brass, because in this temperature range the evaporation time is independent of the surface materials as shown in Fig. 1. The two plates have the same size, 150 mm in dia and 20 mm in thickness, and those surfaces are slightly concaved so that a droplet may not spill off.

The experimental apparatus is shown schematically in Fig. 3. A droplet is deposited softly from the hypodermic syringe (b) to the heated plate (a). The time duration until the droplet disappears after it touched the plate, i.e. the evaporation time τ of droplet, is measured by a stop watch. At the same time, the evaporating droplet is photographed by the strobo-streak camera (h) under the light of strobo-scope (f) and by 8 mm cine-camera (h). From these photographs we can obtain the change in the projected base area A of droplet. Of course, the droplet adheres to or floats over the surface according to the surface temperature T_{w0}. In order to measure the surface temperature T_w just below the evaporating droplet, we use the 0.3 mm dia chromel–alumel sheath type thermocouple (m), as mentioned before. The liquid temperature T_L of droplet is measured with a 25 μm dia chromel–alumel bare type thermocouple (l), fastened at the tip of a bar, the hot junction of which is set up about 0.1 mm over that for T_w-measurement. The droplet falls so as to pass through these two hot junctions. The signals from these two thermocouples, T_w and T_L, are led to the dual-beam synchroscope (j). To measure the temperature T_{w0}, we use two additional thermocouples, and we adopt the mean temperature of the two as T_{w0}. The temperature T_{w0} ranges from 80–450°C in the present experiment.

RESULTS AND DISCUSSION

The heat required to evaporate one droplet, Q, is given by equation (1),

$$Q = (\pi/6)D_0^3\rho(L + L_0). \tag{1}$$

If the initial diameter D_0 and temperature of the droplet are fixed, Q is kept constant. On the other hand, Q is expressed by equation (2),

$$Q = \int_0^\tau \alpha \Delta T A \, dt. \tag{2}$$

The time-averaged heat flux q of the evaporating droplet may be expressed by equation (3),

$$q = Q \Big/ \left(\int_0^\tau A \, dt \right) \tag{3}$$

where

$$\int_0^\tau A \, dt$$

is the time-integration of the projected base area A of the droplet during its life-time, and it can be obtained

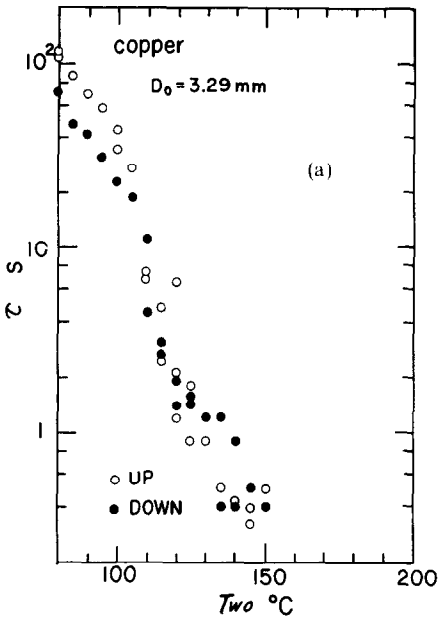

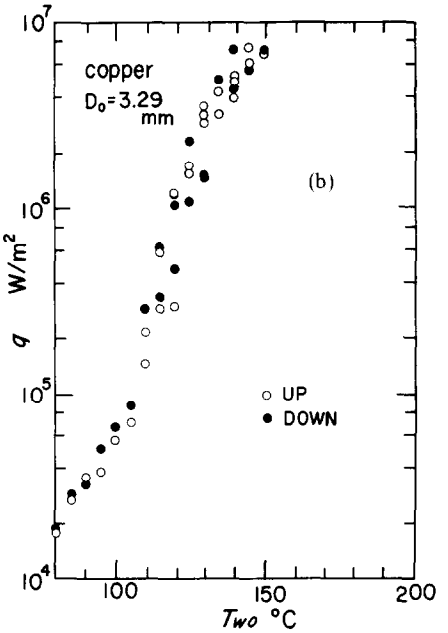

FIG. 4. Effects of the surface condition of copper plate: (a) total evaporation time; (b) time-averaged heat flux.

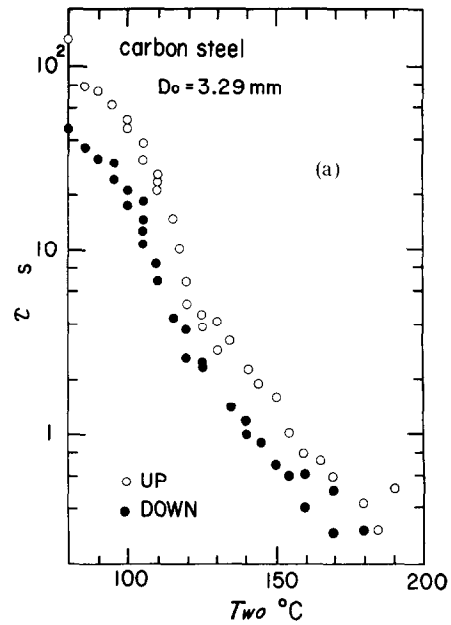

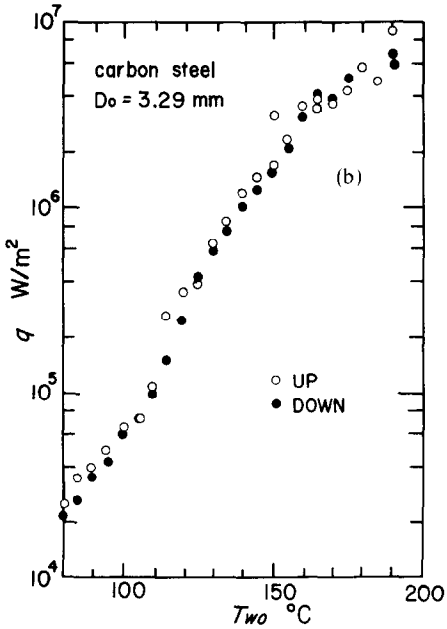

FIG. 5. Effects of the surface condition of carbon steel plate: (a) total evaporation time; (b) time-averaged heat flux.

experimentally as mentioned before. The following expression can be written,

$$\int_0^{\tau} A\,\mathrm{d}t = \bar{A}\tau. \tag{4}$$

1. *In the range of* $T_{w0} < T_F$

1.1. *Effects of surface conditions.* Figure 4(a) shows the evaporation curve, τ vs T_{w0}, for the copper plate and Fig. 5(a) shows that for the carbon steel plate. These figures show that in the case of UP the evaporation time τ is longer than in the case of DOWN at fixed value of T_{w0}. These differences of τ may be due to the wettability of oxidized film on the surface, which governs the time-averaged projected base area $\bar{A}$. Hence, if we correlate the time-averaged heat flux q expressed by equations (3) and (4) with the surface temperature T_{w0}, two curves for UP and DOWN agree well as shown in Figs. 4(b) and 5(b). Since this fact is recognized for each of four materials of the plates, the diagrams of q vs T_{w0} are shown in Fig. 6 without distinction of UP and DOWN. The appearances of the evaporating droplet are illustrated also in this figure, from which it can be seen that the same appearances take place in the range of the same time-averaged heat flux q for any plate materials.

1.2. *Changes in* T_w *and* T_L *with time.* Figure 7 shows examples of changes in T_w and T_L with time obtained by using the dual-beam synchroscope, in which (a) is the case of the brass plate, UP, $T_{w0} = 155°C$, and (b) is

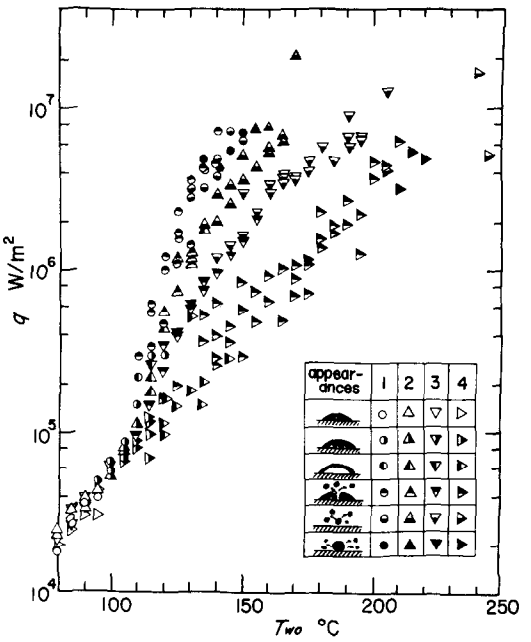

FIG. 6. Time-averaged heat flux vs initial surface temperature for four plate materials: (1) copper; (2) brass; (3) carbon steel; (4) stainless steel.

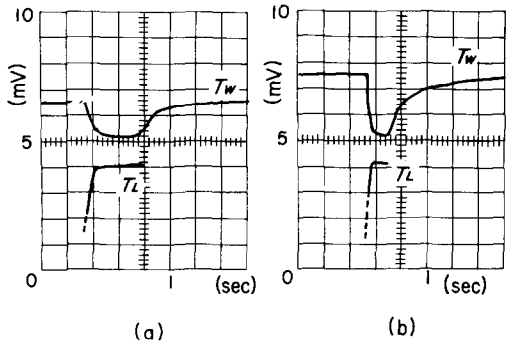

FIG. 7. Changes in T_w and T_L with time obtained by dual-beam synchroscope: (a) brass plate, UP, $T_{w0} = 155°C$; (b) carbon steel, DOWN, $T_{w0} = 185°C$.

the carbon steel plate, DOWN, $T_{w0} = 185°C$. The surface temperature T_w just below the droplet falls considerably immediately after the droplet touched the surface, and then it is kept at almost constant temperature until the droplet disappears on the surface, regardless of the material of the plate. On the other hand, the water temperature T_L of droplet rises, and then it is kept at almost constant temperature, which is nearly equal to the saturation temperature T_{sat}.

The more the thermal diffusivity of the plate material is, the less the temperature drop, ΔT_{drop}. When T_{w0} is lower than T_B, ΔT_{drop} is nearly constant regardless of T_{w0}. This corresponds to the non-boiling region. When T_{w0} is between T_B and T_M, ΔT_{drop} increases with increasing T_{w0}. This corresponds to the nucleate boiling region. If T_{w0} is higher than T_M, ΔT_{drop} takes nearly the same values as the maximum value in the former temperature range. This corresponds to the transition boiling and film boiling region.

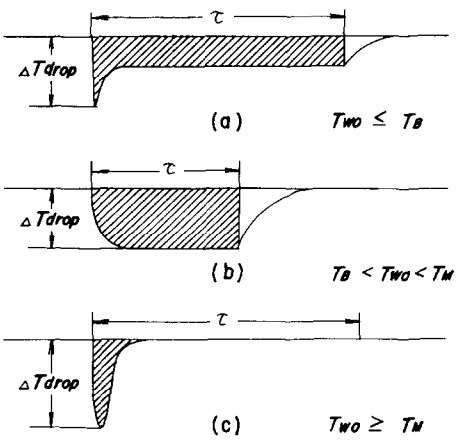

FIG. 8. Schematic diagram of change in T_w with time: (a) $T_{w0} \leqq T_B$; (b) $T_B < T_{w0} < T_M$; (c) $T_M \leqq T_{w0}$.

Such changes of T_w are summarized in Figs. 8(a)–(c). If we subtract the value, that is calculated by dividing the hatched area in Fig. 8 by the evaporation time τ, from T_{w0}, we can obtain the surface temperature T_{ws}. Correlating the time-averaged heat flux q with the surface temperature T_{ws} in place of the initial surface

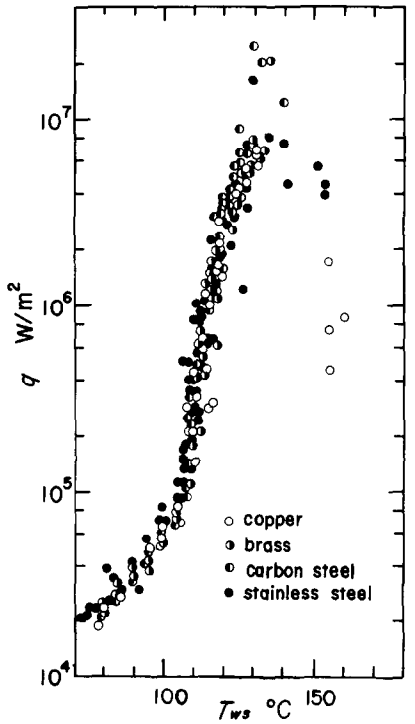

FIG. 9. Time-averaged heat flux q vs T_{ws} for four plate materials.

temperature T_{w0} in Fig. 6, we can obtain Fig. 9. This shows that the whole data for the various plate materials coincide very well. Consequently, Fig. 9 presents the heat-transfer characteristics of a single water droplet of 3.29 mm dia, independently of the surface conditions and surface materials.

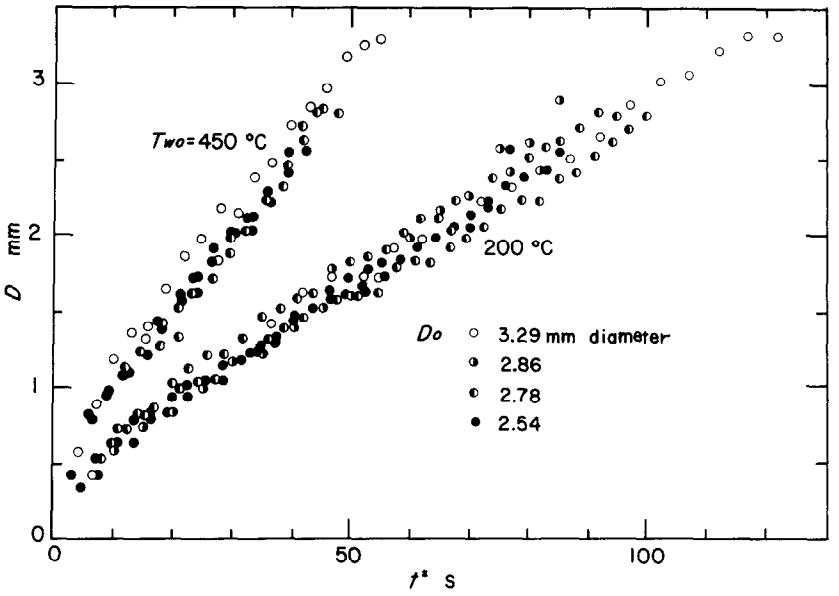

FIG. 10. Instantaneous diameter of droplet obtained from photographs vs reversed time.

2. *In the range of* $T_{w0} > T_F$

The instantaneous diameters of droplet taken from the photographs are presented for two cases, i.e. T_{w0} is 450 and 200°C, in Fig. 10. In this figure the time t^* is reversed to the normal one, i.e. its origin is the time when the droplet just disappeared. Changes in diameter are almost independent of the initial droplet diameter, but they are influenced mainly by T_{w0}. Then we may write the relations between the diameter of droplet D at any time and the reversed time t^* such as equation (5),

$$D = at^{*1/n} \tag{5}$$

where a and n are functions of T_{w0}. Substituting equation (5) into equation (4), we can obtain the time-averaged projected base area $\bar{A}$ by the calculation,

$$\bar{A} = \int_0^\tau A\,dt^*/\tau = (\pi/4)\int_0^\tau D^2\,dt^*/\tau$$
$$= (\pi/4)[n/(n+2)]D_0^2 \tag{6}$$

where $\bar{A}/D_0^2 = (\pi/4)\{n/(n+2)\}$ is independent of the initial droplet diameter D_0.

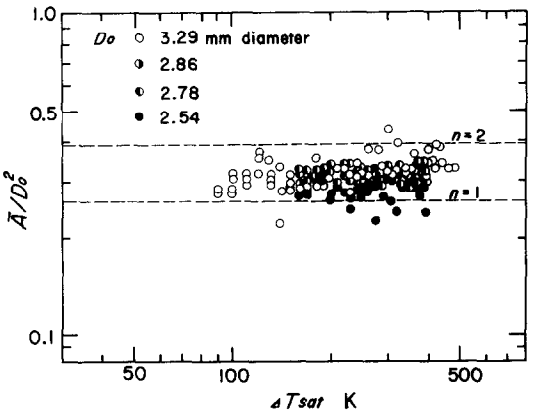

FIG. 11. Relations between $\bar{A}/D_0^2$ obtained from the data and ΔT_{sat}.

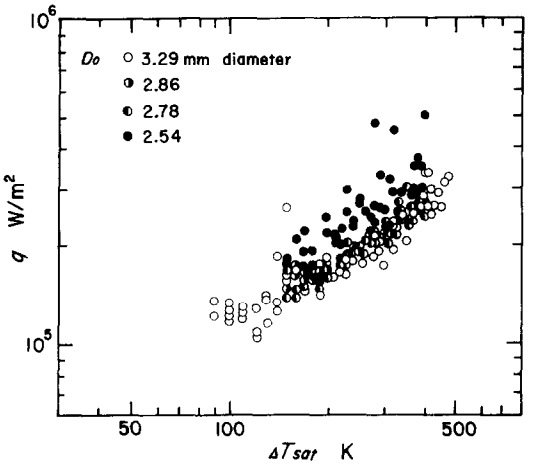

FIG. 12. Time-averaged heat flux q vs ΔT_{sat} for four different initial diameters D_0.

The relation between $\bar{A}/D_0^2$ obtained from the data and ΔT_{sat} ($= T_{w0}$† $- T_{sat}$) is shown in Fig. 11, where the calculated values for $n = 2$ and $n = 1$ in equation (6) are also shown. It can be seen that n exists between 1 and 2, and n is close to 1 for low ΔT_{sat} but it approaches 2 for higher ΔT_{sat}.

On the other hand, the time-averaged heat flux q obtained from the data with equations (3) and (4) is correlated with ΔT_{sat} in Fig. 12, which intimates that the relation between q and ΔT_{sat} is almost independent of the initial droplet diameter D_0. But the data of q for $D_0 = 2.54$ mm are somewhat high. This cause is under investigation.

3. *Boiling curve*

According to the correlation technique mentioned before, we can get the heat-transfer characteristics of a

† In this temperature range, since T_w changes as shown in Fig. 8(c), T_{ws} is nearly equal to T_{w0}.

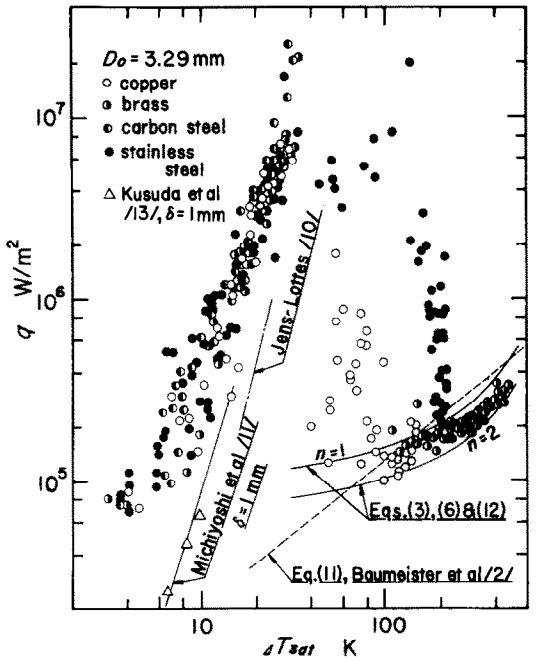

FIG. 13. Boiling curve of a single water droplet of D_0 = 3.29 mm.

single water droplet of 3.29 mm dia for various surface materials of heated plates in the whole temperature range in the present experimental study. The results are shown in Fig. 13. This is the so-called boiling curve.

In the nucleate boiling region the present data provide a straight line parallel to the nucleate pool boiling curve for thin water film of 1 mm thickness on a heated plate of wide area [11, 13], no matter what materials are used for heated plate and no matter how the surface conditions are made. The reason why the present data are located above the nucleate pool boiling curve for thin water film may be due to the violent nucleate boiling in a very small domain of which appearances have already been illustrated in Fig. 6.

In the transition boiling region, the data may be correlated with the same technique as other boiling regions. We deal with two cases of copper and stainless steel plates, because the former has the maximum thermal diffusivity and the latter the minimum in the present experiments. The curve for the stainless steel plate deviates to the higher ΔT_{sat} range than for the copper plate.

In the film boiling region, the relations of q vs ΔT_{sat} are the same as those presented in Fig. 12. But as shown in Fig. 13, ΔT_{sat} at the T_F point is dependent on the surface materials. The higher the thermal diffusivity of the plate, the lower the ΔT_{sat} at the T_F point, as already shown in Fig. 2. Therefore, we get the two different curves for copper and stainless steel in the transition boiling region, but only one curve in the film boiling region regardless of surface materials and surface conditions by virtue of floating of droplet over the surface.

According to the theory of Baumeister *et al.* [2], the heat-transfer coefficient α at any time defined by the projected base area A of droplet in the film boiling region is given by

$$\alpha = 1.1 \times 1.5 \left(\frac{\lambda_v^3 \rho \rho_v L^* g}{\mu_v V^{1/3} \Delta T_{sat}} \right)^{1/4}. \quad (7)$$

On the other hand, the following expression can be derived from the heat balance,

$$-\rho L \frac{dV}{dt} = \alpha(V) A(V) \Delta T_{sat} \quad (8)$$

where V is the volume of droplet at any time. Integration of this equation gives the total evaporation time τ as follows:

$$\tau = \frac{\rho L}{1.1 \times 1.813} \left(\frac{\mu_v}{\lambda_v^3 \rho \rho_v L^* g} \right)^{1/4} \times \Delta T_{sat}^{-3/4} \times \frac{12}{5} V_0^{5/12}. \quad (9)$$

The time-averaged heat-transfer coefficient $\bar{\alpha}$ can be calculated by

$$\bar{\alpha} = \frac{1}{\tau} \int_0^\tau \alpha \, dt = \frac{1}{\tau} \int_{V_0}^0 \alpha(V) \frac{dt}{dV} dV \quad (10)$$

together with equations (7) and (8), and hence it gives the time-averaged heat flux q,

$$q = \bar{\alpha} \Delta T_{sat} = \frac{1.5}{\tau} \times \frac{\rho L}{1.813} \times 3 \times V_0^{1/3} \quad (11)$$

where τ is given by equation (9).

The relationship of q vs ΔT_{sat} thus obtained is also shown in Fig. 13. The present experimental data do not always agree with the theory in the film boiling region. This corresponds to the differences between equation (9) and the present data which are shown in the diagram of τ vs T_{w0} of Fig. 1.

On the other hand, the time-averaged projected base area $\bar{A}$ is given by equation (6), and the total evaporation time τ can be expressed, according to the present experimental data, in the film boiling region by,

$$\tau = 6.25 \times 10^4 \times D_0 \exp(-0.002870 T_{w0}) \quad (12)$$

which is shown in Fig. 1. Since $q = Q/(\bar{A}\tau)$, we can get the relationship between q and ΔT_{sat}. Figure 13 also indicates this relationship which satisfies the present data in the film boiling region if the value of parameter n is 1–2, as already pointed out in Fig. 11.

CONCLUSION

The heat-transfer characteristics of a single droplet of pure water which is placed on smooth surfaces of four plate materials at temperature ranging from 80–450°C are summarized by analysing the so-called boiling curve (q vs ΔT_{sat} diagram, Fig. 13) as follows:

(1) In the nucleate boiling region, the present data provide a straight line parallel to the nucleate pool boiling curve for thin water film, no matter what material is used for heated plate and no matter how surface conditions are made.

(2) In the transition boiling region, the curve for the stainless steel plate comes to higher ΔT_{sat} than for the copper plate, corresponding to the fact that the higher the thermal diffusivity of the plate, the lower the Leidenfrost point T_F, as shown in Fig. 2.

(3) In the film boiling region, the present data provide a certain curve which does not always agree with the theoretical curve derived by Baumeister *et al.* On the other hand, the total evaporation time τ and the time-averaged projected base area of droplet $\bar{A}$ can be expressed by equations (12) and (6), respectively. The time-averaged heat flux q derived from these equations satisfies quite well the present film boiling curve in the whole range of temperature.

REFERENCES

1. B. S. Gottfried, C. J. Lee and K. J. Bell, The Leidenfrost phenomenon: film boiling of liquid droplets on a flat plate, *Int. J. Heat Mass Transfer* **9**, 1167–1187 (1966).
2. K. J. Baumeister, T. D. Hamill and G. J. Schoessow, A generalized correlation of vaporization times of drops in film boiling on a flat plate, in *Proceedings of the Third International Heat Transfer Conference*, Vol. 4, p. 66. A.I.Ch.E., New York (1966).
3. H. Hiroyasu, T. Kadota and T. Senda, Evaporation of a fuel droplet contacting with a hot surface in pressurized and heated ambient gas, *Trans. Japan Soc. Mech. Engrs* **39**(328), 3779–3787 (1973).
4. K. J. Baumeister and F. F. Simon, Leidenfrost temperature—its correlation for liquid metals, cryogens, hydrocarbons, and water, *J. Heat Transfer* **95C**, 166–173 (1973).
5. W. B. Hall, The stability of Leidenfrost drops, in *Proceedings of the Fifth International Heat Transfer Conference*, Vol. 4, pp. 125–129. J.S.M.E.–S.C.E.J., Tokyo (1974).
6. S. Kaji, Bouncing and evaporation of liquid droplets on a heated wall (Dynamic instability of spheroidal state evaporation), *Trans. Japan Soc. Mech. Engrs* **39**(328), 3771–3778 (1973).
7. G. S. Emmerson, The effect of pressure and surface material on the Leidenfrost point of discrete drops of water, *Int. J. Heat Mass Transfer* **18**, 381–386 (1975).
8. S. Kotate, On the evaporation of droplet on hot surface, *Trans. Japan Soc. Mech. Engrs* **36**(287), 1146–1152 (1970).
9. M. Seki, H. Kawamura and K. Sanokawa, Unsteady state heat transfer of impinging droplets—1st Report. Measurements of change in temperature of heated surface, in *Proceedings of the Ninth Japan Heat Transfer Symposium*, pp. 459–462. Heat Transfer Soc. Japan, Tokyo (1972).
10. W. H. Jens and P. A. Lottes, Analysis of heat-transfer burnout, pressure drop and density data for high pressure water, ANL-4627 (1951).
11. I. Michiyoshi and N. Ueno, Heat transfer to thin water film, in *Proceedings of the Ninth Japan Heat Transfer Symposium*, pp. 185–188. Heat Transfer Soc. Japan, Tokyo (1972).
12. L. H. J. Wachters, H. Bonne and H. J. van Nouhuis, The heat transfer from a hot horizontal plate to sessile water drops in the spheroidal state, *Chem. Engng Sci.* **21**, 923–936 (1966).
13. H. Kusuda and K. Nishikawa, Boiling heat transfer in the liquid film (1st Report, The effect of physical properties of the liquid and the condition of the heating surface), *Trans. Japan Soc. Mech. Engrs* **34**(261), 935–943 (1968).

CARACTERISTIQUES DU TRANSFERT THERMIQUE PAR EVAPORATION D'UNE GOUTTE SUR DES SURFACES CHAUDES

Résumé—Cet article présente les caractéristiques du transfert thermique par évaporation d'une goutte unique d'eau pure placée sur des surfaces lisses et chauffées de cuivre, de laiton, d'acier au carbone et d'acier inoxydable à des températures allant de 80 à 450°C. A partir de mesures instantanées de la température de la surface juste sous la goutte et de la variation de la forme de la goutte, sont obtenus le flux thermique moyen q et la température T_{ws} de la surface. On analyse le transfert thermique en reliant le flux q à $\Delta T_{sat} = T_{ws} - T_{sat}$. De cette courbe d'ébullition, on déduit que les résultats obtenus dans la région d'ébullition nucléée en réservoir se placent sur une certaine ligne parallèle à la courbe d'ébullition nucléée pour un film mince d'eau, indépendamment du matériau de la surface chaude, tandis que dans la région de l'ébullition en film, la courbe théorique de Baumeister et al. ne s'accorde pas toujours avec les présents résultats. De nouvelles formules sont présentées pour mieux approcher la courbe d'ébullition en film. On discute aussi l'ébullition de transition.

WÄRMEÜBERGANGSKOEFFIZIENTEN BEI DER VERDAMPFUNG EINES FLÜSSIGKEITSTROPFENS AUF BEHEIZTEN OBERFLÄCHEN

Zusammenfassung—In diesem Bericht werden Wärmeübergangskoeffizienten bei der Verdampfung eines Einzeltropfens aus reinem Wasser auf einer glatten Oberfläche aus Kupfer, Messing, Kohlenstoffstahl und rostfreiem Stahl für einen Temperaturbereich von 80°C bis 450°C angegeben. Aus zeitabhängigen Messungen der Oberflächentemperatur genau unter dem Tropfen und der Änderung der geometrischen Gestalt des Tropfens erhält man den zeitlichen Mittelwert des Wärmestroms q und die Oberflächentemperatur T_{ws}. Die Berechnung der Wärmeübergangs-koeffizienten erfolgt über die Korrelation des Wärmestroms q mit $\Delta T_{sat} = T_{ws} - T_{sat}$. Diese Siedekurve zeigt, daß die vorliegenden Meßergebnisse im Bereich des Blasensiedens in gewisser Weise parallel zur Kurve für das Behälterblasensieden bei dünnem Wasserfilm liegen. Dagegen stimmt im Bereich des Filmsiedens die von Baumeister u.a. theoretisch abgeleitete Kurve nicht immer mit den gewonnenen Meßergebnissen überein. Zur besseren Vorhersage der Kurve für das Filmsieden werden neue Formeln angeben. Das Übergangssieden wird ebenfalls behandelt.

ТЕПЛООБМЕННЫЕ ХАРАКТЕРИСТИКИ ИСПАРЕНИЯ КАПЛИ ЖИДКОСТИ НА НАГРЕТЫХ ПОВЕРХНОСТЯХ

Аннотация — Приводятся теплообменные характеристики испарения единичной капли чистой воды на гладких поверхностях из меди, латуни, углеродистой и нержавеющей стали в диапазоне температур от 80°C до 450°C. Данные об изменении во времени температуры поверхности непосредственно под каплей и геометрической формы капли позволяют получить осредненный по времени тепловой поток q и температуру поверхности T_{ws}. Анализ теплообменных характеристик проводится путем корреляции теплового потока q с $\Delta T_{sat} = T_{ws} - T_{sat}$. Полученная кривая кипения показывает, что данные настоящей работы, снятые в области пузырькового кипения, ложатся на линию, параллельную кривой пузырькового кипения тонкой водяной пленки независимо от материала поверхности нагрева, в то время как в области пленочного кипения теоретическая кривая, полученная Баумайстером и др., не всегда совпадает с полученными в настоящей работе данными. Представлены новые формулы для более точного расчёта кривой пленочного кипения. Рассматривается также и переходный режим кипения.